Attenuation Correction Using Count-Limited Transmission Data in Positron Emission Tomography

Steven R. Meikle, Magnus Dahlbom and Simon R. Cherry

Department of Nuclear Medicine, Royal Prince Alfred Hospital, Sydney, Australia and Division of Nuclear Medicine and Biophysics, UCLA School of Medicine, Los Angeles, California

Poisson noise in transmission data can have a significant influence on the statistical uncertainty of PET measurements, particularly at low transmission count rates. In this paper, we investigate the effect of transmission data processing on noise and quantitative accuracy of reconstructed PET images. Differences in spatial resolution between emission and transmission measurements due to transmission data smoothing are shown to have a significant influence on quantitative accuracy and can lead to artifacts in the reconstructed image. In addition, the noise suppression of this technique is insufficient to greatly reduce transmission scan times. Based on these findings, improved strategies for processing count-limited transmission data have been developed, including a method using segmentation of attenuation images. Using this method, accurate attenuation correction can be performed using transmission scan times as low as 2 min without increasing noise in reconstructed PET images.

J Nucl Med 1993; 34:143–144

The ability to directly measure and correct for photon attenuation makes positron emission tomography (PET) an inherently quantitative procedure, enabling the rates of biochemical processes to be determined in vivo. Attenuation correction can be performed using an external (transmission) source since the probability of attenuation is independent of source position along the line of response (LOR) joining two detectors. Transmission measurements, typically acquired for 20–30 min, are compared with a blank scan, performed without the patient in the tomograph. The ratio of blank to transmission counts gives the attenuation correction factors (ACF) for each LOR. In theory, this provides a perfect correction for photon attenuation, but in practice the technique is limited by noise in the transmission measurement (*1,2*). This is particularly so for LORs passing through the center of the chest, where a 40-fold decrease in detected counts compared with the blank scan is typical.

Of the methods suggested for reducing noise in transmission scans (*2*), sinogram smoothing is most commonly employed. While this is effective in minimizing noise propagation, it can also degrade the quantitative accuracy of PET images (*3*). However, the effect of transmission processing on the accuracy of cardiac PET scans has not been investigated. Such an investigation may lead to alternate methods of transmission processing which improve the accuracy of PET images.

Improved methods of transmission processing may be particularly important in applications where it is impractical to acquire a statistically adequate transmission dataset. Whole body PET imaging (*4*) is such a situation. Imaging is performed at multiple axial positions for 2–4 min at each position, enabling whole body images of the distribution of [^{18}F]fluorodeoxyglucose (FDG) and [^{18}F] fluoride ion to be obtained (*5,6*). Since an adequate transmission dataset cannot be obtained in a practical time frame, attenuation correction is not normally applied. Without suitable techniques for processing count-limited transmission data, the technique is limited to qualitative imaging and is subject to attenuation artifacts.

A boundary attenuation correction method has been suggested for use in cardiac PET studies (*7*). This has the potential to greatly reduce acquisition time for transmission scanning without increasing noise in the ACFs. However, the technique is time-consuming as it requires the operator to manually draw regions of interest (ROIs) on attenuation images corresponding to the lungs and body outline. Recently, a segmented attenuation correction (SAC) method was described (*8*) which allows regions to be automatically assigned using image segmentation. This technique is practical and can reduce the transmission scan time to 10 min with comparable accuracy to a 30 min transmission scan. However, the method would be more effective if the constraints of the discrete anatomic regions into which the images are segmented were relaxed. This could be justified for two reasons. First, not all anatomic regions can be classified as a particular tissue type. For example, the hylar regions of the lung have

Received Dec. 16, 1991; revision accepted Aug. 6, 1992.

For correspondence and reprints contact: Steven Meikle, Department of Nuclear Medicine, Royal Prince Alfred Hospital, Missenden Road, Camperdown, NSW 2050, Australia.

attenuation values that fall between those of lung and soft tissue. Second, the task is to reduce noise in the ACFs, not to classify the attenuation images. Therefore, it is not important for the segmented image to contain discrete anatomic regions.

In this study, optimal methods for processing count-limited transmission data have been investigated and the limitations of such methods assessed. First, the nature and magnitude of errors in attenuation correction due to transmission processing were investigated, with particular reference to cardiac and whole body PET. A modified SAC method was developed and compared with conventional transmission smoothing in the count-limited situation using chest phantom data. Finally, the processing strategies developed in this work were applied to cardiac and whole body PET studies performed on human volunteers and patients.

MATERIALS AND METHODS

Computer Simulations

The computer phantoms were designed with realistic activity and attenuation distributions to simulate a cardiac PET scan (Fig. 1). The myocardium was rotated 15° relative to the vertical axis of the phantom and located so that the lateral wall bordered on the left mid-lung. Transmission and attenuated emission projections were calculated by forward-projection, resulting in sinograms with 256 angular projections, 192 samples per projection and sample spacing of 0.31 cm. These parameters were chosen to simulate data acquired on an ECAT 931/08-12 PET scanner (CTI/Siemens, Knoxville, TN). Finite detector resolution was approximated by convolving the projections with a one-dimensional Gaussian kernel. Random noise, calculated from a Gaussian distribution approximating poisson noise (with pixel variance equal to the pixel count value), could also be added to the projections. After attenuation correction using the simulated transmission data, the emission distribution was reconstructed into a 128 × 128 matrix using filtered backprojection.

Effect of Transmission Processing on the Accuracy of Attenuation Correction

Since transmission processing can affect the resolution of transmission data, we first investigated the effect of differences in emission and transmission resolution on the accuracy of attenuation correction. The simulated emission distribution was forward-projected, attenuated according to the attenuation image and convolved with a one-dimensional Gaussian to simulate 10 mm resolution full width at half maximum (FWHM). The attenuation image was also forward-projected, but resolution was varied to give transmission sinograms with <5 mm resolution FWHM (in this case no blurring was applied but some loss of resolution is expected due to sampling), 10 mm, 15 mm and 20 mm. No noise was added to emission or transmission sinograms. The emission data were corrected for attenuation using each of the transmission sinograms and the results reconstructed using a ramp filter cut off at the Nyquist frequency.

The effect of transmission processing on the accuracy of attenuation correction was examined in a separate simulation experiment. Emission and transmission sinograms were calculated and smoothed to simulate 5.4 mm resolution. After smoothing, noise was added to the transmission data to approximate a 20 min scan obtained with a ring source containing approximately 0.2 mCi per ring (total counts = 24 million). Noise was also added to a constant valued sinogram matrix to approximate a 30 min blank scan (total counts = 74 million). No noise was added to the emission data.

Initially, the following processing was applied to the transmission data:

1. No processing.
2. Smoothed once with a one-dimensional kernel (9 point).
3. Smoothed twice with the same kernel.
4. Smoothed once with a two-dimensional kernel (9 × 9).
5. Smoothed twice with the same kernel.

The one-dimensional and two-dimensional smoothing kernels approximate a Gaussian distribution with FWHM of 11 mm. When applied twice, the effective FWHM is 15.6 mm. The latter is the smoothing that is normally applied to blank and transmission sinograms for attenuation correction of cardiac PET scans. In each case, the blank scan was processed by smoothing with the two-dimensional Gaussian. The attenuation corrected emission data were reconstructed using a ramp filter cut off at the Nyquist frequency.

In addition to the above, a segmentation algorithm was implemented and applied to the reconstructed attenuation images. The segmented images were forward-projected and used to calculate ACFs. This processing yields transmission data with resolution approaching the ideal case, resulting in resolution mismatch between the emission sinogram and the forward-projected transmission sinogram. To test the effect of this on the accuracy of

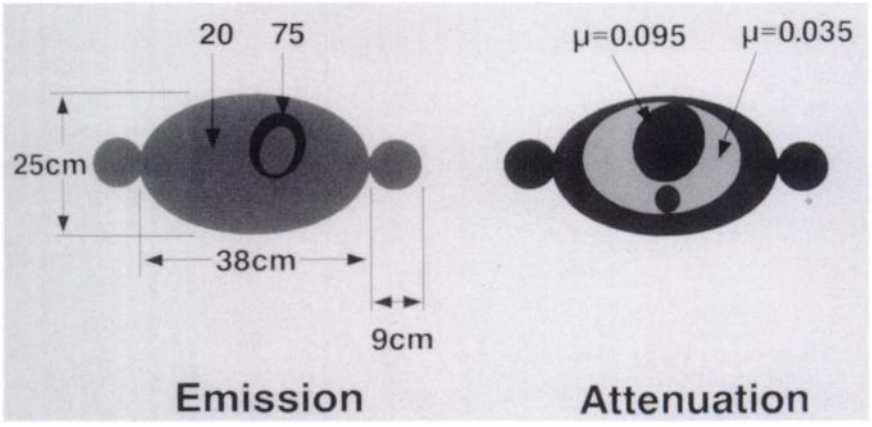

FIGURE 1. Geometry of computer simulated chest phantom showing simulated activity and attenuation values.

the method, the processing was performed twice. In the second case, the forward-projected sinogram was convolved with a one-dimensional Gaussian kernel (FWHM = 5.4 mm) to correct for the difference in resolution. The segmentation algorithm is described in detail in the following section.

Description of the Modified SAC Algorithm

Attenuation images are reconstructed by taking the log of the ratio of blank to transmission counts. No smoothing or other processing is applied to either the blank or transmission sinograms prior to this step. Images are reconstructed into 128 × 128 matrices using a Shepp windowed ramp filter, with roll-off at the Nyquist frequency. A high-resolution reconstruction filter is chosen to circumvent errors in lung boundary definition due to loss of resolution. The values in these matrices read directly as attenuation coefficients in units of cm^{-1}. To improve the signal-to-noise ratio (SNR) in the unprocessed images, a median filter is applied in-plane and axially. This filter has the property that it achieves some degree of noise suppression but maintains resolution across boundaries (*9*). For each image, the histogram of attenuation values is calculated (Fig. 2) and three peaks corresponding to air, lung and soft tissue are identified. For low count transmission data, some image smoothing is usually required. The smoothing operation is performed only to aid in the identification of the peaks. The unprocessed images are used for the following steps.

Gaussian functions are fitted to each of the three peaks in the histogram. The choice of function was based on observation of the attenuation histogram in several patient studies. Although for the peak corresponding to air, the choice was somewhat arbitrary, the other two peaks in each case were found to closely approximate Gaussian functions. For each Gaussian, a cumulative probability density function (PDF) is calculated by integrating under the curve up to the point where the maximum value occurs. Thus, a point has maximum likelihood of belonging to the peak when it lies exactly on the peak and decreasing likelihood as distance from the peak increases. The probabilities of a given pixel value, μ, belonging to the peaks corresponding to air, lung and soft tissue—$P(\mu_{air}|\mu)$, $P(\mu_{lung}|\mu)$ and $P(\mu_{st}|\mu)$ respectively—are calculated from the PDF. Then, the pixel's new value, μ', is calculated as:

$$\mu' = \frac{1}{N}\left(\mu_{air} \times P(\mu_{air}|\mu) + \mu_{lung} \times P(\mu_{lung}|\mu) + \mu_{st} \times P(\mu_{st}|\mu)\right)$$

where

$$N = P(\mu_{air}|\mu) + P(\mu_{lung}|\mu) + P(\mu_{st}|\mu).$$

Thus, a continuous range of μ values is possible in the segmented image. To remove spurious pixel values, a two-dimensional median filter is applied to the segmented image. Once the image is processed, it is forward-projected to form a transmission sinogram. ACFs can either be calculated directly during the forward-projection step or following forward-projection by reference to a noiseless blank scan.

The forward-projected transmission sinogram can be smoothed to match the resolution of the emission sinogram to which attenuation correction will be applied. For simulated data, the blurring function required to achieve matched resolution is known. For real data, however, the FWHM of the required blurring function may be different to the intrinsic detector resolution used in the simulated case. To test this, a 1.4 mm diameter ^{68}Ge line source, positioned 1 cm off axis in the ECAT 931 scanner, was measured and simulated. The simulated line source was forward-projected and convolved with a Gaussian function with FWHM equal to the intrinsic detector resolution. Both data were reconstructed into a 128 × 128 matrix with pixel size of 0.8 mm using a ramp filter cut off at the Nyquist frequency. The reconstructed resolution was 5.8 ± 0.5 mm and 6.2 ± 0.5 mm (FWHM) for the measured and simulated line sources respectively. The difference is negligible indicating that a blurring function equal to the intrinsic detector resolution is appropriate for both simulated and real data.

The following phantom and human studies were performed on a ECAT 931/08-12 tomograph. The scanner is equipped with a ring transmission source (ring diameter = 65 cm) which contained approximately 0.2 mCi of ^{68}Ge per ring at the time these studies were performed. The scanner has a detector diameter of 102 cm and sensitivity of approximately 155 $kcounts \cdot sec^{-1} \cdot \mu Ci^{-1} \cdot ml^{-1}$ for a 20 cm cylinder.

Attenuation Correction Using Count-Limited Transmission Data

An elliptical phantom was used to assess the count limitations of attenuation correction using these processing methods. The phantom measures 36 cm in the major axis, 21 cm in the minor axis and has a depth of 25 cm. A cylindrical cardiac insert was placed in the center of the phantom which has an outer diameter of 8 cm and wall thickness of 0.9 cm. Another cylinder of diameter 10.5 cm containing a low density foam similar to lung ($\mu \cong 0.03\ cm^{-1}$) was placed adjacent to the cardiac insert. A section of polystyrene foam ($\mu \cong 0.01\ cm^{-1}$) was shaped to surround both the lung cylinder and part of the cardiac insert. The myocardial chamber was filled with water containing 0.89 $\mu Ci \cdot ml^{-1}$ of ^{18}F. The central chamber and the remainder of the phantom were filled with water containing 0.14 $\mu Ci \cdot ml^{-1}$ of ^{18}F.

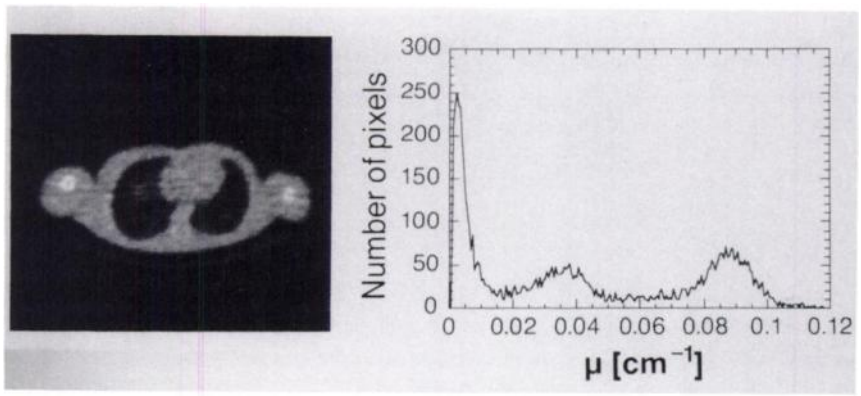

FIGURE 2. Attenuation image and its histogram. The three main peaks due to air, lung and soft tissue are clearly seen. Note the extent to which the three distributions overlap.

These activities were chosen to give approximately a 6:1 ratio between the myocardium and the background.

A dynamic emission scan consisting of 12 × 5 min frames followed by 6 × 10 min frames was acquired. By summing frames, an emission dataset typical of a 20 min cardiac scan (total counts per plane = 1 million) was formed. The phantom was left in position to decay over a 15 hr period and a transmission scan performed without moving the phantom. The transmission study was also acquired as a dynamic dataset, consisting of 5 × 1 min frames, 5 × 5 min frames, 1 × 30 min and 1 × 20 min to give a total acquisition time of 3 hr. The frames were summed to form transmission datasets with acquisition times ranging from 1 min to 30 min. In addition, all frames were summed to form a single, high statistic transmission scan of 3 hr. A typical 30 min blank scan as well as a high statistics, 2 hr blank scan were also acquired.

Attenuation correction of the 20 min emission data was performed using 1–30 min transmission data processed using two-dimensional sinogram smoothing and modified SAC. The emission data were reconstructed into a 128 × 128 matrix using a Shepp filter with roll-off at 0.3× the Nyquist frequency. Attenuation correction was also performed using the high statistics blank and transmission data without any processing and reconstructed using the same filter.

Human Studies

A cardiac PET study was performed on a healthy male volunteer with no history of cardiac disease. First, a dynamic blank scan was acquired, consisting of 2 × 30 min frames. These were summed to form a 30 min and a 1 hr blank scan. A dynamic transmission scan, consisting of 2, 8, 10 and 70 min frames was acquired. These frames were summed to form a short transmission scan of 2 min, a typical transmission scan of 20 min and a high statistics transmission scan of 90 min duration. The patient was then administered 20 mCi of ^{13}N-ammonia intravenously and a 20 min static scan was acquired after a 10-min delay. Following this, 10 mCi of ^{18}FDG were administered intravenously and, after a 30 min delay, a 20 min static scan was acquired. The ^{13}N-ammonia and ^{18}FDG scan data were corrected for attenuation with the transmission smoothing method using the 20 min transmission data and with the modified SAC method using both the 2 min and 20 min transmission data. The emission scan was also corrected using the high statistics blank and transmission data without any processing. All images were reconstructed into a 128 × 128 matrix with 1.5 mm pixels using a Shepp filter with roll-off at 0.3× the Nyquist frequency, yielding reconstructed resolution of approximately 11 mm (FWHM).

The methods described have been further validated in whole body PET studies performed on a healthy male volunteer and two patients undergoing routine investigations. One patient was a female with known breast carcinoma and metastatic disease, the other a female with known ovarian carcinoma. Transmission data were acquired for 4 min at each of the 8 axial positions without interleaving to give an axial field of view (FOV) of 80 cm, plane separation of 6.75 mm and a total acquisition time of 32 min. Following intravenous administration of 10 mCi of ^{18}FDG and a 30 min delay for tracer equilibration, emission data were acquired for 2 min each at 16 axial positions with interleaving of consecutive datasets to give an axial FOV of 80 cm, plane separation of 3.375 mm and a total acquisition time of 32 min. Axial interpolation of the transmission data was performed to match the finer sampling of the emission data. Emission data were processed using: (a) no attenuation correction, (b) measured attenuation correction using sinogram smoothing and (c) modified SAC. In each case, emission data were reconstructed using a Shepp filter with roll-off at 0.3× the Nyquist frequency, resulting in reconstructed resolution of 11 mm.

RESULTS

Effect of Transmission Processing on the Accuracy of Attenuation Correction

The effect of mismatched resolution between emission and transmission data is demonstrated in Figure 3. When resolution is matched (image B), the resulting PET image has uniform background and uniform myocardial counts, as expected. When resolution is mismatched, artifacts are seen in the reconstructed images at the borders between soft tissue and lung. Horizontal count profiles taken at a level through the middle of the myocardium reveal the effect on the quantitative level in the myocardium. When transmission resolution is better than emission resolution (e.g., when transmission data are derived from segmented attenuation images), counts on the soft tissue side of the interface are artificially increased, resulting in overestimation of lateral wall counts. When transmission resolution is worse than emission resolution (e.g., when the transmission sinogram is smoothed), the effect is reversed and counts in the lateral wall are underestimated.

A semi-automated ROI analysis was performed on the PET images. ROIs were defined for six sectors corresponding to the infero-lateral, lateral, antero-lateral, anterior, antero-septal and septal segments. Reconstructed counts were compared with the same sectors on the image in which no attenuation was present and the calculated errors are presented in Table 1. The largest error was measured in the lateral wall (−7.6%) using the transmission data with 20 mm resolution.

Figure 4 shows images obtained by processing transmission data using the various methods outlined in the methods section. As expected, smoothing the blank scan alone

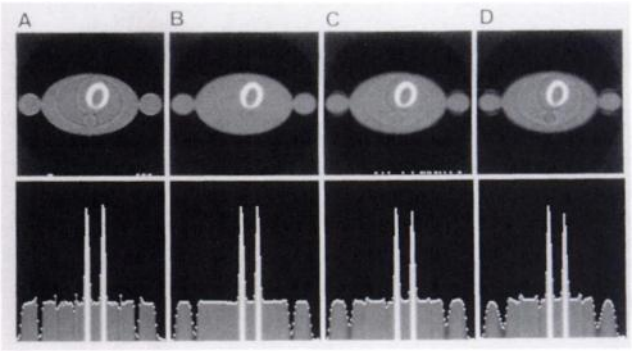

FIGURE 3. Effect of mismatched resolution between emission and transmission data. Simulated transmission resolution is: (A) <5 mm FWHM, (B) 10 mm FWHM, (C) 15 mm FWHM and (D) 20 mm FWHM. In each case, the emission resolution is 10 mm FWHM. Therefore, resolution is matched in image B only. The bottom row are horizontal count profiles at a mid level through the myocardium, corresponding to the images in the top row.

TABLE 1
Errors in Attenuation Correction Due to Mismatched Resolution*

Sector†	Transmission resolution‡ (FWHM) <5 mm§	10 mm	15 mm	20 mm
SEP	0%	0%	−1.2%	−1.2%
A-SEP	0%	0%	0%	0%
ANT	0%	0%	0%	0%
A-LAT	+2.7%	0%	−2.7%	−4.0%
LAT	+3.8%	−1.3%	−5.0%	−7.6%
I-LAT	+4.1%	−1.4%	−4.1%	−6.8%

* Expressed as percent errors calculated by comparison with control image in which no attenuation was present.

† Cardiac segments are septal (SEP), antero-septal (A-SEP), anterior (ANT), anterolateral (A-LAT), lateral (LAT) and infero-lateral (I-LAT).

‡ Emission resolution was 10 mm FWHM in all cases.

§ No blurring was applied to these transmission data. However, some loss of resolution is expected due to finite sampling.

TABLE 2
Errors in Attenuation Correction Due to Transmission Data Processing*

Sector†	Processing method‡ a	b	c
SEP	−1.1%	−3.5%	−1.1%
A-SEP	+0.1%	−3.7%	+0.1%
ANT	−2.2%	−3.4%	−3.5%
A-LAT	−11.0%	+0.2%	−3.5%
LAT	−13.2%	+4.7%	−0.9%
I-LAT	−11.9%	−1.4%	−3.7%

* Expressed as percent errors calculated by comparison with control image in which no attenuation was present.

† Cardiac segments are septal (SEP), antero-septal (A-SEP), anterior (ANT), anterolateral (A-LAT), lateral (LAT) and infero-lateral (I-LAT).

‡ Processing methods used were: (a) two-dimensional smoothing with effective FWHM 16 mm; (b) segmentation; (c) segmentation with smoothing after forward-projection to account for mismatched resolution.

(image B) has little effect on noise in the reconstructed image. By using both one-dimensional and two-dimensional smoothing operations on the transmission data (images C–F), artifacts are seen at the soft tissue/lung borders, similar to those in Figure 3. The artifacts become worse with increased smoothing and are more apparent when two-dimensional smoothing is applied compared with one-dimensional smoothing. Similarly, if forward-projected transmission sinograms are not smoothed following segmentation (image G) to account for mismatched resolution, artifacts similar to those in Figure 3 arise. These artifacts are eliminated by smoothing the high resolution transmission sinogram to achieve matched resolution (image H).

Semi-automated ROI analysis was performed on the images obtained by two-dimensional smoothing, segmentation with mismatched resolution and segmentation with matched resolution. The calculated errors for the cardiac sectors are shown in Table 2. The error in the lateral wall is −13.2% by applying two-dimensional smoothing twice.

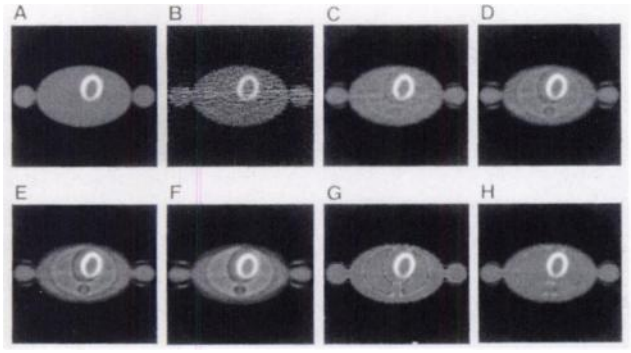

FIGURE 4. Effect of transmission data processing on the accuracy of attenuation correction. (A) Control image in which no attenuation was applied to the simulated data. Processing performed on the remaining images is: (B) smooth blank scan only, (C) one-dimensional smooth on transmission sinogram once, (D) one-dimensional smooth twice, (E) two-dimensional smooth once, (F) two-dimensional smooth twice, (G) segmentation with mismatched resolution and (H) segmentation with matched resolution.

Attenuation Correction Using Count-limited Transmission Data

A subset of the reconstructed PET images, corrected for attenuation using 1–30 min transmission data and the attenuation images before and after segmentation are shown in Figure 5. The images processed using transmission smoothing appear acceptable using transmission data acquired for 10 min but rapidly deteriorate for acquisition times below 10 min. The modified SAC method successfully processed transmission data down to and including the 2 min study, with good differentiation between water, foam/bed (which have similar μ values) and air. The emission images resulting from this method of transmission processing appear equally acceptable for transmission data acquired for 2 to 30 min. The 1 min image is slightly noisier than the others.

The mean reconstructed count and its standard deviation were calculated for a ROI over the uniform background area. The quantitative error was calculated by comparison with the same ROI drawn on the study reconstructed using attenuation correction with the high statistics transmission data and no transmission processing. This error was plotted against transmission scan time for the sinogram smoothing and modified SAC methods (Fig. 6).

Human Studies

The results of the volunteer cardiac study are shown in Figure 7. The first row shows the attenuation image reconstructed from the 90 min transmission scan without any

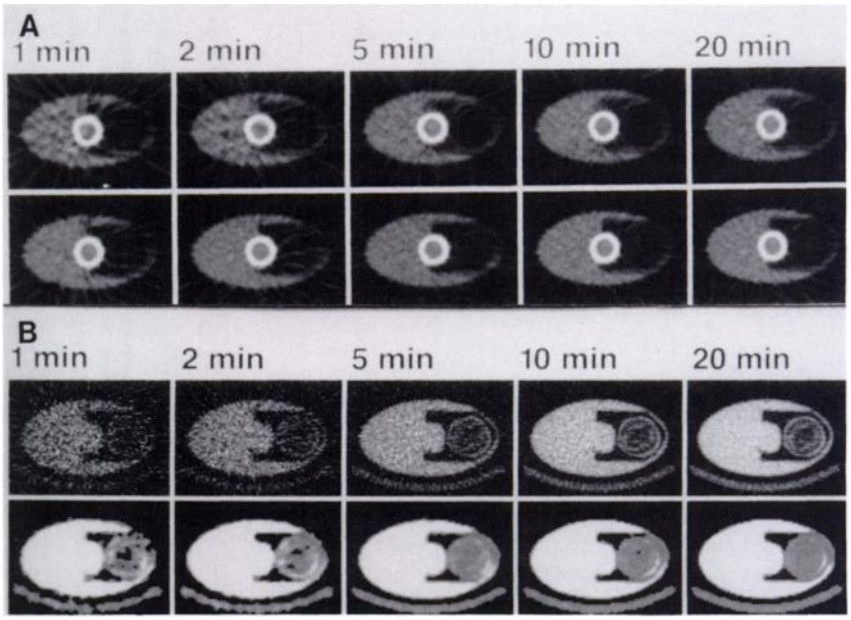

FIGURE 5. Reconstructed images of the chest phantom using transmission scans ranging from 1 min to 20 min for attenuation correction. The top row is processed using transmission smoothing. The bottom row is processed using the modified SAC method. (B) The reconstructed attenuation images (top row) and the segmented attenuation images (bottom row).

processing, the attenuation image reconstructed following smoothing of the 20 min transmission scan, the segmented 20 min attenuation image and the segmented 2 min attenuation image. Shown on the second and third rows are the reconstructed ^{13}N-ammonia and ^{18}FDG images respectively, processed using the corresponding transmission data in the first row. There is no noticeable difference in image quality between the images using 2 min transmission data by segmentation and those using 20 min data. The ^{13}N-ammonia image obtained by transmission smoothing is more heterogeneous than those obtained using the high count transmission data and segmentation, with an appreciable reduction in the lateral and infero-lateral walls (indicated by the arrows). In the ^{18}FDG images, there is enhancement of glucose utilization in the lateral wall and relatively reduced utilization in the anterior segment in both the high count transmission image and the images obtained by segmentation, consistent with recent findings in the normal human heart (*10*). These regional variations are less apparent on the image obtained by transmission smoothing.

Coronal sections obtained from the reconstructed whole body PET images are shown in Figure 8 for each of the three studies performed. In each row, the first image is obtained without attenuation correction, the second image is obtained by using measured attenuation correction with sinogram smoothing, and the third image is obtained by using modified SAC. In each case, image artifacts, such as enhanced peripheral and lung field activity, are eliminated by attenuation correction using both methods. However, image SNR is appreciably degraded using conventional transmission processing, whereas image quality is apparently preserved using modified SAC. No artifacts or false-positives were introduced as a result of modified SAC processing of transmission data.

DISCUSSION

The results of the spatial resolution experiment suggest that a difference in intrinsic resolution between emission and transmission measurements has a significant effect on the accuracy of attenuation correction. When spatial averaging is applied to transmission sinograms, the resolution mismatch is quite significant, particularly considering the heavy smoothing that is normally applied. On the ECAT 931, the final transmission resolution after smoothing is approximately 17 mm compared with 5–6 mm for the emission data. We have shown that such a large resolution mismatch leads to loss of quantitative accuracy and artifacts in reconstructed PET images, particularly in regions which are in close proximity to a lung/soft tissue interface. These artifacts are of particular importance in cardiac PET imaging due to the intimate proximity of the lateral and infero-lateral myocardial walls to the left mid-lung, as illustrated in Figure 7. While the emission data used in this example was common to each processing method, it is possible that subject motion during the latter part of the 90 min transmission scan could account for some of the differences noted. This was excluded by comparing the latter 70 min of this study with the first 20 min. Therefore, the differences are attributed to the type of transmission processing alone. These artifacts will not only lead to errors in quantifying blood flow or glucose utilization, but will also cause apparently nonuniform uptake in the myocardium which may, using visual analysis of the images, lead to misinterpretation of the study. The calculation of polar maps by reference to a normal data base (*11*) may overcome this problem. We note that the problem of mismatched resolution would not arise if the same smoothing was applied to the emission data. While this will degrade the resolution of the emission data, it may be possible to use a smaller (less smooth) kernel in conjunction with a

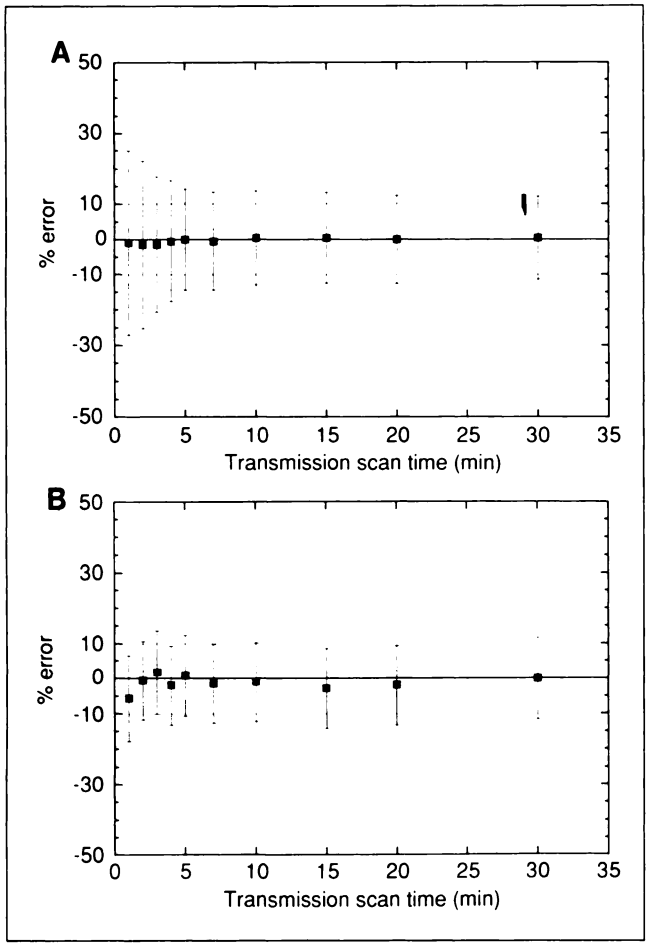

FIGURE 6. Plot of quantitative error in a uniform region of the chest phantom versus transmission scan time using two-dimensional smoothing (A) and modified SAC (B) as the method of transmission processing. The error bars represent the noise (% standard deviation) in the ROI measurement.

sharper reconstruction filter to maintain reconstructed resolution.

The artifacts in the myocardium may be of less concern in whole body PET imaging. We found that using transmission smoothing, the transmission scan time could be reduced by a factor of two without affecting image quality appreciably. However, for attenuation correction of whole body PET images, greater reduction in transmission scan time is required. Therefore, a segmentation algorithm was implemented and evaluated which is applied to reconstructed attenuation images. Based on our earlier findings, smoothing was applied to the sinograms calculated by forward projection. This is necessary since segmentation yields attenuation images which approach infinite resolution, resulting in mismatched resolution between acquired emission sinograms and forward-projected transmission sinograms. Smoothing was applied by convolving the forward-projected sinograms with a Gaussian kernel with FWHM equal to the intrinsic resolution of the detector. We found that the additional degradation due to interpolation during forward-projection is negligible. Therefore, this method results in resolutions which are approximately matched.

By using the segmentation algorithm and appropriate filtering, the feasibility of performing attenuation correction using transmission scans acquired for as little as 2 min was demonstrated, both in a phantom study and in a human volunteer. The modified SAC method was also applied to whole body ^{18}FDG PET studies and shown to allow attenuation correction of these count-limited studies without any appreciable reduction in image quality. Attenuation correction in whole body PET imaging enables the technique to be used for dosimetry calculations in biodistribution studies (*12*). Some further investigation is required to fully develop quantitative whole body PET. For example, attenuation correction could be made more prac-

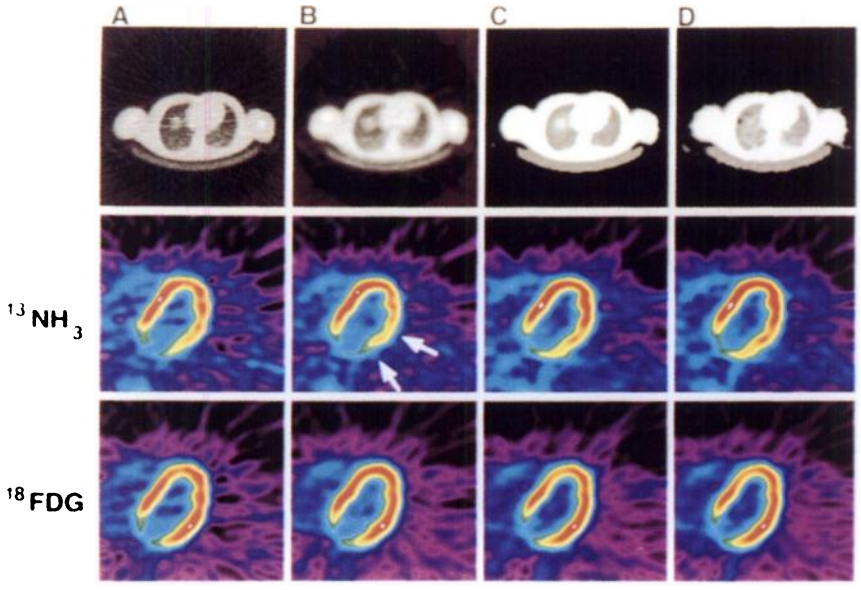

FIGURE 7. Nitrogen-13-ammonia (middle row) and ^{18}FDG (bottom row) study in a normal, healthy volunteer. Images were processed using the attenuation data in the top row. The processing used was: (A) long transmission scan with no processing, (B) two-dimensional smoothing of transmission data, (C) segmentation of 20-min transmission data and (D) segmentation of 2-min transmission data.

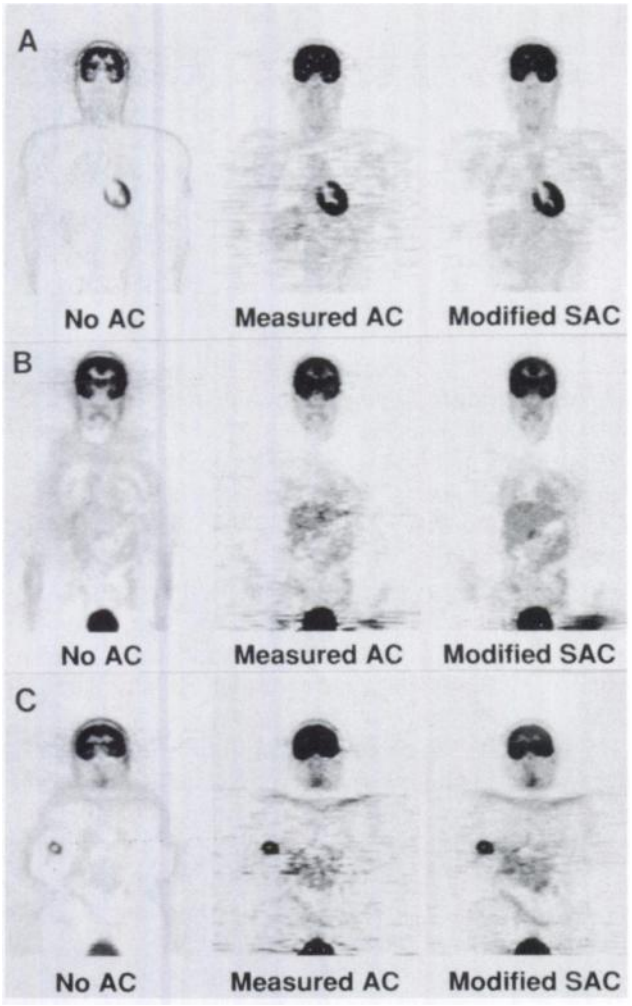

FIGURE 8. Coronal sections from whole body ^{18}FDG PET studies performed on a male volunteer (A), a female patient with ovarian carcinoma (B) and a female patient with known breast carcinoma (C). Images were obtained using no attenuation correction (AC) (1st column), measured AC with sinogram smoothing (2nd column) and modified SAC (3rd column).

tical if emission and transmission data were acquired simultaneously (*13–15*). In addition, noninterleaved transmission data were used in this study to allow the acquisition time to be doubled at each axial position. The data were then interpolated in the axial direction before being applied to interleaved emission data. The effect of axial sampling and filtering of transmission data will require further investigation.

CONCLUSION

In this paper, we have demonstrated the effect of transmission data processing on the accuracy of attenuation correction and the importance of maintaining matched emission and transmission resolution. Mismatched resolution due to transmission smoothing causes attenuation artifacts which can account for signal suppression of up to 13% on the soft tissue side of a soft tissue/lung interface and which preferentially affects the lateral wall in myocardial PET studies. In addition, transmission smoothing alone cannot achieve sufficient noise suppression to allow greatly reduced transmission scan times. We have implemented and evaluated a segmentation method for application in the count-limited transmission situation. Following segmentation of attenuation images, transmission sinograms are calculated by forward-projection and convolved with a one-dimensional Gaussian to match resolution to the intrinsic resolution of emission data. The methods developed in this work allow accurate attenuation correction to be performed using transmission scans acquired for as little as 2 min without significantly affecting the signal-to-noise level in reconstructed PET images.

ACKNOWLEDGMENTS

The authors thank Stefan Siegel, Arion Chatziioannou, Edward J. Hoffman and Sung-Cheng Huang for their contributions during discussions on aspects of this work. We also thank Ron Sumida for scheduling time on the scanner and arranging the volunteer studies. This work was supported by the Australian Nuclear Science & Technology Organization, Department of Energy contract DE-FC03-87-ER 60615 and National Institutes of Health grants R01-HL33177-07 and R01-HL29845-08.

REFERENCES

1. Huang SC, Hoffman EJ, Phelps ME, Kuhl DE. Quantitation in positron emission tomography: 2. Effect of inaccurate attenuation correction. *J Comput Assist Tomogr* 1979;3:804–814.
2. Dahlbom M, Hoffman EJ. Problems in signal-to-noise ratio for attenuation correction in high resolution PET. *IEEE Trans Nucl Sci* 1987;34: 288–293.
3. Palmer MR, Rogers JG, Bergstrom M, Beddoes MP, Pate BD. Transmission profile filtering for positron emission tomography. *IEEE Trans Nucl Sci* 1986;33:478–481.
4. Guerrero TM, Hoffman EJ, Dahlbom M, Cutler PD, Hawkins RA, Phelps ME. Characterization of a whole body imaging technique for PET. *IEEE Trans Nucl Sci* 1990;37:676–680.
5. Hoh CK, Maddahi J, Glaspy J, et al. PET total body imaging of breast cancer with FDG and F-18 ion [Abstract]. *J Nucl Med* 1991;32:981.
6. Hoh CK, Maddahi J, Glaspy J, et al. Total body PET imaging of the abdomen and pelvis with FDG [Abstract]. *J Nucl Med* 1991;32:982.
7. Huang SC, Carson R, Phelps M, Hoffman E, Schelbert H, Kuhl D. A boundary method for attenuation correction in positron emission tomography. *IEEE Trans Nucl Sci* 1981;22:627–637.
8. Xu EZ, Mullani NA, Gould KL, Anderson WL. A segmented attenuation correction for PET. *J Nucl Med* 1991;32:161–165.
9. Gonzalez RC, Wintz P. *Digital image processing.* Addison-Wesley; 1987:162–163.
10. Hicks RJ, Herman WH, Kalff V, et al. Quantitative evaluation of regional substrate metabolism in the human heart by positron emission tomography. *J Am Coll Cardiol* 1991;18:101–111.
11. Hicks K, Ganti G, Mullani N, Gould KL. Automated quantitation of three-dimensional cardiac positron emission tomography for routine clinical use. *J Nucl Med* 1989;30:1787–1797.
12. Hoffman EJ. Quantitation of radiopharmaceutical distribution for use in dose estimates with positron emission tomography. *Proceedings of fourth international radiopharmaceutical dosimetry symposium.* Oak Ridge, TN: 1985:97–104.
13. Thompson CJ, Ranger NT, Evans AC. Simultaneous transmission and emission scans in positron emission tomography. *IEEE Trans Nucl Sci* 1989;36:1011–1016.
14. Ranger NT, Thompson CJ, Evans AC. The application of a masked orbiting transmission source for attenuation correction in PET. *J Nucl Med* 1989;30:1056–1068.
15. Thompson CJ, Ranger N, Evans AC, Gjedde A. Validation of simultaneous PET emission and transmission scans. *J Nucl Med* 1991;32:154–160.